

Central residues in prion protein PrP^C are crucial for its conversion into the pathogenic isoform

Received for publication, March 9, 2022, and in revised form, August 8, 2022. Published, Papers in Press, August 13, 2022.
<https://doi.org/10.1016/j.jbc.2022.102381>

Agriani Dini Pasiana^{1,†}, Hironori Miyata^{2,†}, Junji Chida¹, Hideyuki Hara¹, Morikazu Imamura³,
Ryuichiro Atarashi³, and Suehiro Sakaguchi^{1,*}

From the ¹Division of Molecular Neurobiology, The Institute for Enzyme Research (KOSOKEN), Tokushima University, Tokushima, Japan; ²Animal Research Center, School of Medicine, University of Occupational and Environmental Health, Yahatanishi, Kitakyushu, Japan; ³Division of Microbiology, Department of Infectious Diseases, Faculty of Medicine, University of Miyazaki, Kiyotake, Miyazaki, Japan

Edited by Elizabeth Coulson

Conformational conversion of the cellular prion protein, PrP^C, into the amyloidogenic isoform, PrP^{Sc}, is a key pathogenic event in prion diseases. However, the conversion mechanism remains to be elucidated. Here, we generated Tg(PrP Δ 91-106)-8545/*Prnp*^{0/0} mice, which overexpress mouse PrP lacking residues 91-106. We showed that none of the mice became sick after intracerebral inoculation with RML, 22L, and FK-1 prion strains nor accumulated PrP^{Sc} Δ 91-106 in their brains except for a small amount of PrP^{Sc} Δ 91-106 detected in one 22L-inoculated mouse. However, they developed disease around 85 days after inoculation with bovine spongiform encephalopathy (BSE) prions with PrP^{Sc} Δ 91-106 in their brains. These results suggest that residues 91-106 are important for PrP^C conversion into PrP^{Sc} in infection with RML, 22L, and FK-1 prions but not BSE prions. We then narrowed down the residues 91-106 by transducing various PrP deletional mutants into RML- and 22L-infected cells and identified that PrP mutants lacking residues 97-99 failed to convert into PrP^{Sc} in these cells. Our *in vitro* conversion assay also showed that RML, 22L, and FK-1 prions did not convert PrP Δ 97-99 into PrP^{Sc} Δ 97-99, but BSE prions did. We further found that PrP mutants with proline residues at positions 97 to 99 or charged residues at positions 97 and 99 completely or almost completely lost their converting activity into PrP^{Sc} in RML- and 22L-infected cells. These results suggest that the structurally flexible and noncharged residues 97-99 could be important for PrP^C conversion into PrP^{Sc} following infection with RML, 22L, and FK-1 prions but not BSE prions.

Prions are proteinaceous infectious particles causing prion diseases, a group of devastating neurodegenerative disorders, including Creutzfeldt-Jakob disease (CJD) in humans and scrapie and bovine spongiform encephalopathy (BSE) in animals (1, 2). They are widely believed to consist, if not entirely, of the abnormally folded, amyloidogenic isoform of prion protein, designated PrP^{Sc}, which is produced from the cellular

isoform of prion protein, PrP^C, through conformational conversion (1, 2). PrP^C is a glycoprotein tethered to the outer cell membrane *via* a glycosylphosphatidylinositol anchor moiety and expressed most abundantly in the brain, particularly by neurons (1, 2). It has been assumed that, upon prion infection, PrP^{Sc} interacts with PrP^C, forcing it to undergo conformational conversion into PrP^{Sc} *via* a seeded protein polymerization mechanism, resulting in propagation of PrP^{Sc} or prions. Indeed, mice devoid of PrP^C (*Prnp*^{0/0}) have been shown to be resistant to prion infections, neither propagating PrP^{Sc} or prions in their brains nor developing disease even after intracerebral inoculation with the prions (3–6), strongly arguing that the conformational conversion of PrP^C into PrP^{Sc} is a key pathogenic event in prion diseases.

Many reverse genetic studies using reconstituted *Prnp*^{0/0} mice with transgenes encoding various mutant PrPs have been reported to elucidate the conversion mechanism of PrP^C into PrP^{Sc} and have identified specific sites or amino acid residues in PrP^C that are involved in the conversion of PrP^C into PrP^{Sc} (7–11). We previously generated Tg(PrP Δ 91-106)/*Prnp*^{0/0} mice, which express mouse PrP lacking residues 91-106, or PrP Δ 91-106, on the *Prnp*^{0/0} background as low as only 0.4-fold levels of PrP^C in wildtype (WT) mice (12). PrP Δ 91-106 was predominantly localized at the lipid raft domains of the plasma membrane, similarly to WT PrP^C, in mouse neuroblastoma N2a cells and in the brains of Tg(PrP Δ 91-106)/*Prnp*^{0/0} mice (12). Tg(PrP Δ 91-106)/*Prnp*^{0/0} mice were markedly resistant to mouse-adapted RML, 22L, FK-1, and BSE prions. They developed disease with a very long incubation time of 538 \pm 24 days postinoculation (dpi) with BSE prions with accumulation of PrP^{Sc} Δ 91-106 in their brains, while remained healthy without accumulation of PrP^{Sc} Δ 91-106 in their brains up to at least 604 dpi with FK-1 prions, 765 dpi with RML scrapie prions, and 623 dpi with 22L scrapie prions (12). These results suggested that residues 91-106 could be involved in prion pathogenesis in a strain-dependent manner. However, it remains unclear whether the reduced susceptibility of Tg(PrP Δ 91-106)/*Prnp*^{0/0} mice to these prions is due to the low expression of PrP Δ 91-106 or the lack of residues 91-106 or both. It also remains unknown how residues 91-106 are

[†] These authors contributed equally to this work.

* For correspondence: Suehiro Sakaguchi, sakaguchi@tokushima-u.ac.jp.

Central residues crucial for prion protein conversion

involved in the conversion of PrP^C into PrP^{Sc} in prion infection.

In this study, we generated a new line of Tg(PrPΔ91-106)/Prnp^{0/0} mice, designated Tg(PrPΔ91-106)-8545/Prnp^{0/0} mice, which overexpress PrPΔ91-106 in their brains 6-times as high as PrP^C in WT mice and intracerebrally inoculated RML, 22L, FK-1, and BSE prions into them. None of the RML, 22L, or FK-1 prion-inoculated Tg(PrPΔ91-106)-8545/Prnp^{0/0} mice became sick up to at least 337 dpi, without PrP^{Sc}Δ91-106 accumulation in their brains except for very small amounts of PrP^{Sc}Δ91-106 detected in one 22L prion-inoculated brain specimen. However, they developed disease at 85 ± 4 dpi with BSE prions with PrP^{Sc}Δ91-106 accumulation in their brains. These results clearly indicate that residues 91-106 are crucial for PrP^C to convert into PrP^{Sc} in infection with RML, 22L, and FK-1 prions but not BSE prions. We then narrowed down residues 91-106 by transducing various PrP mutants into RML- and 22L-infected cells, identifying that residues 97-99 are important for PrP^C to convert into PrP^{Sc} in infection with RML and 22L prions. *In vitro* protein misfolding cyclic amplification (PMCA) assay also showed that residues 97-99 are important for RML, 22L, and FK-1 prions, but not for BSE prions, to induce the conversion of recombinant PrP into PrP^{Sc}. We also found that PrP mutants with proline residues at positions 97 to 99 or charged residues at positions 97 and 99 completely or almost completely lost their converting activity into PrP^{Sc} in RML- and 22L-infected cells, suggesting that the structural flexibility and noncharged properties might be important for residues 97-99 to mediate the conversion of PrP^C into PrP^{Sc} in infection with RML and 22L prions.

Results

Generation of Tg(PrPΔ91-106)-8545/Prnp^{0/0} mice

To clarify the role of residues 91-106 of PrP^C in prion infection, we newly generated a PrPΔ91-106-overexpressing line of Tg(PrPΔ91-106)/Prnp^{0/0} mice, termed Tg(PrPΔ91-106)-8545/Prnp^{0/0} mice. We noticed that Tg(PrPΔ91-106)-8545/Prnp^{0/0} mice expressed PrPΔ91-106 at very high levels in their brains. Therefore, to estimate the exact expression levels

of PrPΔ91-106 in their brains, we diluted Tg(PrPΔ91-106)-8545/Prnp^{0/0} brain homogenates with Prnp^{0/0} brain homogenates 5 and 10 times and compared the signal densities of PrPΔ91-106 in these homogenates to those of PrP^C in undiluted C57BL/6 WT brain homogenates on Western blotting with IBL-N anti-PrP antibodies, which were raised against the N-terminal peptide of PrP. PrPΔ91-106 was clearly detected in the brains of Tg(PrPΔ91-106)-8545/Prnp^{0/0} mice (Fig. 1A). It migrated faster than WT PrP^C due to the deletion of residues 91-106, with three major bands similar to WT PrP^C, each corresponding to diglycosylated, monoglycosylated, and non-glycosylated forms (Fig. 1A). By densitometric analysis after taking into account the dilution factors of Tg(PrPΔ91-106)-8545/Prnp^{0/0} brain homogenates, PrPΔ91-106 was estimated to be expressed in the brains of Tg(PrPΔ91-106)-8545/Prnp^{0/0} mice at levels about 6-times higher than PrP^C in WT mice (Fig. 1B). On inspection, no obvious developmental and growth abnormalities were observed in Tg(PrPΔ91-106)-8545/Prnp^{0/0} mice up to about 2 years after birth, suggesting that PrPΔ91-106 might not be toxic *in vivo*.

High resistance of Tg(PrPΔ91-106)-8545/Prnp^{0/0} mice to RML, 22L, and FK-1 prions but not to BSE prions

We then intracerebrally inoculated RML, 22L, FK-1, and BSE prions into Tg(PrPΔ91-106)-8545/Prnp^{0/0} mice as well as C57BL/6 WT mice as controls. WT mice developed disease at 167 ± 4, 149 ± 2, 152 ± 7, and 180 ± 5 dpi with RML, 22L, FK-1, and BSE prions, respectively (Table 1). Tg(PrPΔ91-106)-8545/Prnp^{0/0} mice were highly resistant to RML, 22L, and FK-1 prions, displaying no abnormal clinical signs at least up to 358 dpi with RML prions and 337 dpi with 22L and FK-1 prions (Table 1). In contrast, they developed disease at 85 ± 4 dpi with BSE prions (Table 1). We also investigated PrP^{Sc}Δ91-106 in the brains of Tg(PrPΔ91-106)-8545/Prnp^{0/0} mice inoculated with RML, 22L, FK-1, and BSE prions by Western blotting with SAF61 anti-PrP antibody, which recognizes residues 141-152 of mouse PrP (13). PrP^{Sc} was detected in the brains of ill WT mice inoculated with RML, 22L, FK-1, and BSE prions (Fig. 2, A–D). However, no

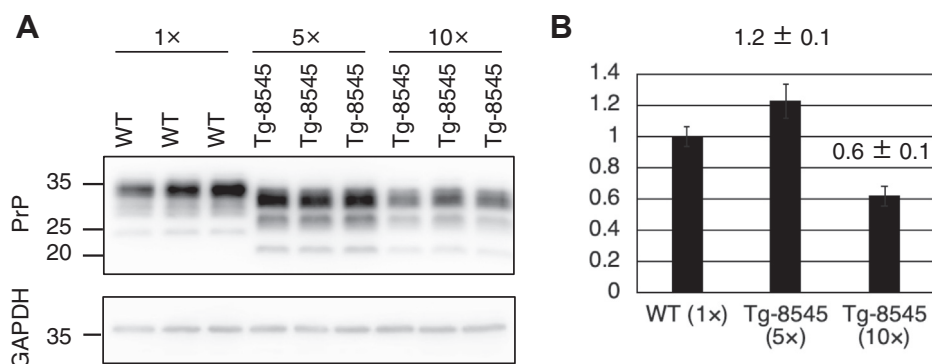


Figure 1. PrPΔ91-106 expression in the brains of Tg(PrPΔ91-106)-8545/Prnp^{0/0} mice. A, Western blotting with IBL-N anti-PrP antibodies of brain homogenates from 8- to 10-week-old C57BL/6 WT (n = 3) and Tg(PrPΔ91-106)-8545/Prnp^{0/0} mice (n = 3). The Tg(PrPΔ91-106)-8545/Prnp^{0/0} brain homogenates were diluted 5- (5x) and 10-times (10x) with brain homogenates from Prnp^{0/0} mice. Glyceraldehyde-3-phosphate dehydrogenase (GAPDH) is an internal control. B, signal densities for WT PrP^C and PrPΔ91-106 in (A) were measured. The ratio of the PrPΔ91-106 densities against the WT PrP^C densities were then calculated after normalization against the GAPDH densities.

Table 1

Incubation times in WT and Tg(PrP Δ 91-106)-8545/Prnp^{0/0} mice inoculated with RML, 22L, FK-1, and BSE prions

Prions	Recipient mouse	Expression level of PrP (fold) ^a	Diseased mice /Total mice	Times to the onset of disease (Days \pm SD)	p value (log-rank test)
RML	WT	1	11/11	167 \pm 4	<0.0001
	Tg(PrP Δ 91-106)-8545/Prnp ^{0/0}	6.0	0/7	>358	
22L	WT	1	10/10	149 \pm 2	<0.0001
	Tg(PrP Δ 91-106)-8545/Prnp ^{0/0}	6.0	0/7	>337	
FK-1	WT	1	10/10	152 \pm 7	<0.0001
	Tg(PrP Δ 91-106)-8545/Prnp ^{0/0}	6.0	0/7	>337	
BSE	WT	1	10/10	180 \pm 5	<0.0001
	Tg(PrP Δ 91-106)-8545/Prnp ^{0/0}	6.0	8/8	85 \pm 4	

^a Expression levels of mutant PrP were compared to those of PrP^C in WT mice using Western blotting.

PrP^{Sc} Δ 91-106 was detectable in the brains of asymptomatic Tg(PrP Δ 91-106)-8545/Prnp^{0/0} mice, which were sacrificed at 358 dpi with RML prions and 337 dpi with 22L and FK-1 prions, except for very faint signals for PrP^{Sc} Δ 91-106

detected in one 22L-inoculated Tg(PrP Δ 91-106)-8545/Prnp^{0/0} mouse (Fig. 2, A–C). In contrast, PrP^{Sc} Δ 91-106 was observed in the brains of BSE-inoculated, ill Tg(PrP Δ 91-106)-8545/Prnp^{0/0} mice (Fig. 2D). Compared to WT PrP^{Sc}, PrP^{Sc} Δ 91-106

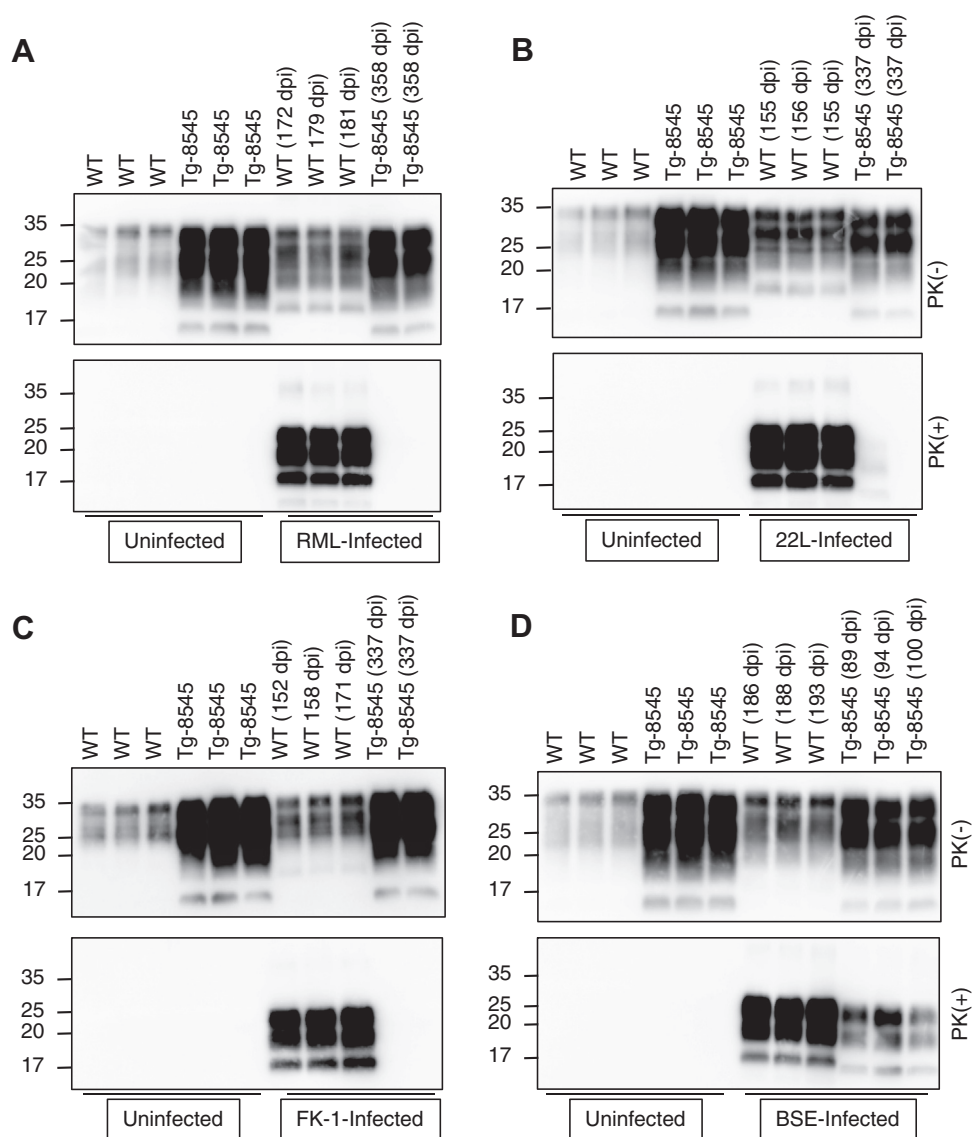


Figure 2. PrP^{Sc} Δ 91-106 in the brains of prion-inoculated Tg(PrP Δ 91-106)-8545/Prnp^{0/0} mice. Western blotting with SAF61 anti-PrP antibody of brain homogenates from C57BL/6 WT and Tg(PrP Δ 91-106)-8545/Prnp^{0/0} mice intracerebrally inoculated with or without RML (A), 22L (B), FK-1 (C), and BSE prions (D). Brain homogenates from uninfected mice were used as controls. Date of the sacrifice of BSE-, RML-, 22L-, and FK-1-inoculated WT and Tg(PrP Δ 91-106)-8545/Prnp^{0/0} mice were shown in parenthesis. BSE, bovine spongiform encephalopathy.

Central residues crucial for prion protein conversion

had lower levels (Fig. 2D). This is consistent with the fact that overexpression of PrP in the brain results in low production of PK-resistant PrP after prion infection (7). Taken together, these results indicate that residues 91-106 could be crucial for PrP^C to convert into PrP^{Sc} following infection with RML, 22L, and FK-1 prions but not BSE prions, therefore Tg(PrP^Δ91-106)-8545/*Prnp*^{0/0} mice being highly resistant to RML, 22L, and FK-1 prions but not to BSE prions.

Identification of residues 97-99 as being crucial for PrP^C to convert into PrP^{Sc} after infection with RML and 22L prions

To investigate the mechanism of how residues 91-106 are involved in the conversion of PrP^C into PrP^{Sc} in prion infection, we determined to identify the residue(s) within residues 91-106 that are crucial for PrP^C to convert into PrP^{Sc} in RML- and 22L-infected cells. To do this, we first investigated whether residues 91-106 are important for PrP^C to convert into PrP^{Sc} in RML- and 22L-infected cells, by transducing an expression vector encoding PrP^Δ91-106 with the 3F4 epitope or PrP^Δ91-106(3F4), into RML- and 22L-infected mouse neuroblastoma N2a cells, termed N2aC24Chm and N2aC24L1-3 cells, respectively. Both infected cells were previously established by incubating N2aC24 cells, which is a clone of N2a cells persistently overexpressing exogenously transduced mouse PrP^C, with brain homogenates from RML- and 22L-infected mice and subjecting them to limiting dilution cloning (14). The 3F4 epitope, which is widely used to distinguish transduced PrPs from endogenous PrP^C, locates closely to residue 106 (15), raising the concern that deletion of residue 106 might disrupt the 3F4 epitope, thereby making it impossible to detect PrP^Δ91-106 on Western blotting with 3F4 antibody. Therefore, we transduced PrP^Δ91-106(3F4) as well as PrP^Δ91-105(3F4) and PrP^Δ91-104(3F4) into N2aC24Chm and N2aC24L1-3 cells. 3F4 antibody detected PrP^Δ91-104(3F4), with slightly lower signal densities than those of WT PrP^C(3F4), but not PrP^Δ91-106(3F4) and PrP^Δ91-105(3F4) (Fig. 3, A and B), indicating that the 3F4 epitope is disrupted by deletion of residues 105 or 106 but only partially by deletion of residue 104. However, no PrP^{Sc}Δ91-104(3F4) was observed in N2aC24Chm and N2aC24L1-3 cells transduced with PrP^Δ91-104(3F4) (Fig. 3, A and B), indicating that residues 91-104 are important for PrP^C to convert into PrP^{Sc} in RML- and 22L-infected cells.

We then investigated whether PrP^Δ91-104(3F4) could have a transdominant-negative inhibitory activity against the conversion of endogenous PrP^C into PrP^{Sc}. Western blotting with SAF61 anti-PrP antibody, which detects endogenous PrP^C and PrP^Δ91-104(3F4), showed that total amounts of PrP were 6.9 and 6.4-times higher in WT PrP^C(3F4)- and PrP^Δ91-104(3F4)-transduced N2aC24Chm cells and 2.1-times in both WT PrP^C(3F4)- and PrP^Δ91-104(3F4)-transduced N2aC24L1-3 cells, respectively, than those in empty vector-transduced, control N2aC24Chm and N2aC24L1-3 cells (Fig. 3, C and D). These results indicate that WT PrP^C(3F4) and PrP^Δ91-104(3F4) are expressed at levels much higher than or

comparable to that of endogenous PrP^C in N2aC24Chm and N2aC24L1-3 cells, respectively, ruling out the possibility that PrP^Δ91-104(3F4) might be insufficiently expressed and therefore fail to convert into PrP^{Sc}Δ91-104(3F4) in N2aC24Chm and N2aC24L1-3 cells. PrP^{Sc} was lower in PrP^Δ91-104(3F4)-transduced N2aC24Chm than in empty vector- or WT PrP^C(3F4)-transduced N2aC24Chm cells (Fig. 3C). Transfection with lower amounts of the expression vector (2 μg *versus* 5 μg) for PrP^Δ91-104(3F4) downregulated the expression of PrP^Δ91-104(3F4) and did not reduce PrP^{Sc} in N2aC24Chm cells (Fig. S1). Consistent with this, PrP^Δ91-104(3F4)-transduced N2aC24L1-3 cells, which expressed the lower levels of PrP^Δ91-104(3F4), exhibited no PrP^{Sc} reduction (Fig. 3D). Neither increased expression of PrP^Δ91-104(3F4) nor reduced PrP^{Sc} were observed in N2aC24L1-3 cells even after transfection with higher amounts of the expression vector (10 μg *versus* 5 μg) for PrP^Δ91-104(3F4) (Fig. S2). Taken together, these results suggest that PrP^Δ91-104(3F4) could transdominantly inhibit the conversion of endogenous PrP^C into PrP^{Sc} in an expression level-dependent manner.

We then transduced expression vectors encoding a series of PrP mutants with various deletions within residues 91-104, such as PrP^Δ91-96(3F4), PrP^Δ91-100(3F4), PrP^Δ96-100(3F4), PrP^Δ96-104(3F4), and PrP^Δ100-104(3F4), into N2aC24Chm and N2aC24L1-3 cells. Western blotting with 3F4 antibody showed that only PrP^Δ91-96(3F4) was converted into PrP^{Sc}Δ91-96(3F4) in these cells (Fig. 4, A and B), suggesting that residues other than residues 91-96 are important for the conversion of PrP^C into PrP^{Sc}. However, PrP^Δ100-104(3F4) was hyperglycosylated due to a newly created N-glycosylation site consisting of residues 99(N), 105(K), and 106(T) (Fig. 4, A and B), suggesting the possibility that the unsuccessful conversion of PrP^Δ100-104(3F4) into PrP^{Sc}Δ100-104(3F4) is due to the glycosylation not due to the deletion of residues 100-104. To address this, we transduced an expression vector encoding PrP^Δ100-103(3F4), whose deletion does not create a glycosylation site, into N2aC24Chm and N2aC24L1-3 cells. PrP^Δ100-103(3F4) was converted into PrP^{Sc}Δ100-103(3F4) in both cells (Fig. 4, C and D), indicating that the glycosylation in PrP^Δ100-104(3F4) is responsible for its unsuccessful conversion into PrP^{Sc}Δ100-104(3F4) and that residues 100-103 are dispensable for PrP^C to convert into PrP^{Sc} in infection with RML and 22L prions. Residues 97-99 are missing in the conversion-incompetent PrP^Δ91-104(3F4), PrP^Δ91-100(3F4), PrP^Δ96-100(3F4), and PrP^Δ96-104(3F4) but intact in the conversion-competent PrP^Δ91-96(3F4) and PrP^Δ100-103(3F4). It is thus possible that residues 97-99 could be important for PrP^C to convert into PrP^{Sc} following infection with RML and 22L prions. To confirm this, we transduced PrP mutants with deletion of each residue at positions 97 to 99, termed PrP^Δ97(3F4), PrP^Δ98(3F4), and PrP^Δ99(3F4), into N2aC24Chm and N2aC24L1-3 cells. PrP^Δ97(3F4), PrP^Δ98(3F4), and PrP^Δ99(3F4) were not converted into PrP^{Sc} (Fig. 4, E and F), further supporting that residues 97-99 could play an important role for the conversion of PrP^C into PrP^{Sc} in infection with RML and 22L prions.

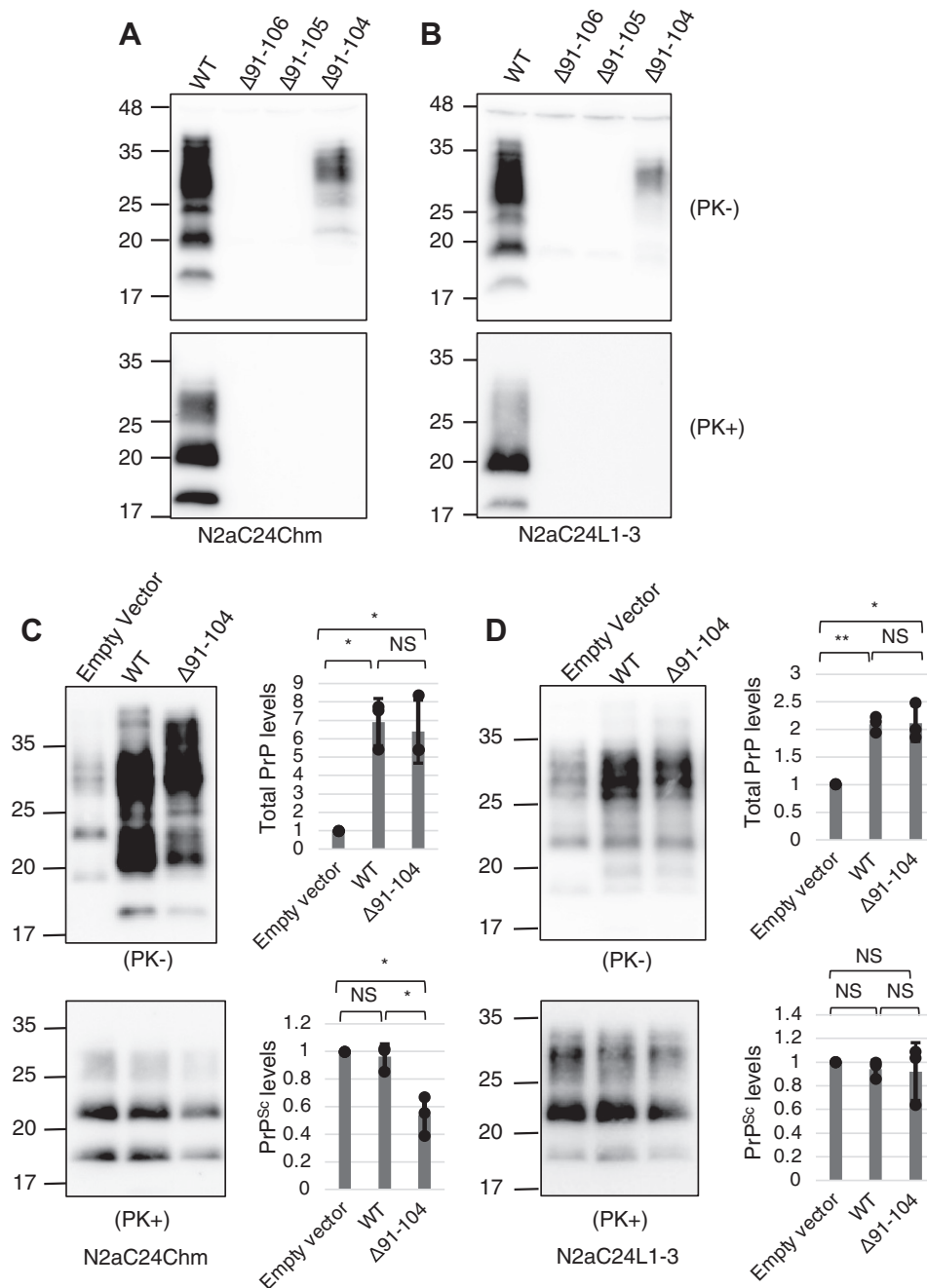


Figure 3. Disruption of 3F4 epitope by deletion of residue 106 or 105. Western blotting with 3F4 anti-PrP antibody of the lysates from N2aC24Chm (A) and N2aC24L1-3 cells (B) transduced with expression vectors encoding WT PrP^C(3F4), PrP Δ 91-106(3F4), PrP Δ 91-105(3F4), or PrP Δ 91-104(3F4) after treatment with (+) or without (-) PK. Western blotting with SAF61 anti-PrP antibody of the lysates from N2aC24Chm (C) and N2aC24L1-3 cells (D) transduced with control empty expression vector or expression vectors encoding WT PrP^C(3F4) or PrP Δ 91-104(3F4) after treatment with (+) or without (-) PK. Total PrP levels and PrP^{Sc} levels in WT PrP^C(3F4)- or PrP Δ 91-104(3F4)-transduced N2aC24Chm and N2aC24L1-3 cells were compared to those in control empty vector-transduced N2aC24Chm and N2aC24L1-3 cells. Data were from independent triplicate experiments. NS, not significant; **p* < 0.05, ***p* < 0.01 (Student's *t* test).

PrP Δ 97-99 is converted into PrP^{Sc} Δ 97-99 in a PMCA assay with BSE prions but not with RML, 22L, and FK-1 prions

N2a cells or N2a cells overexpressing PrP^C are susceptible to RML, 22L, and FK-1 prions (14, 16–18), but not to BSE prions. Therefore, to investigate the role of residues 97-99 in the strain-dependent conversion of PrP^C into PrP^{Sc}, we performed an *in vitro* PMCA assay with baculovirus-derived recombinant

mouse WT PrP and PrP Δ 97-99 by incubating with brain homogenates from RML-, 22L-, FK-1-, and BSE-infected WT mice. Consistent with our previous results (12), Western blotting of the PK-treated PMCA products showed that WT PrP was converted into PrP^{Sc} after incubation with prion-infected brain homogenates to various degrees in a strain-dependent manner (Fig. 5). However, PrP Δ 97-99 was

Central residues crucial for prion protein conversion

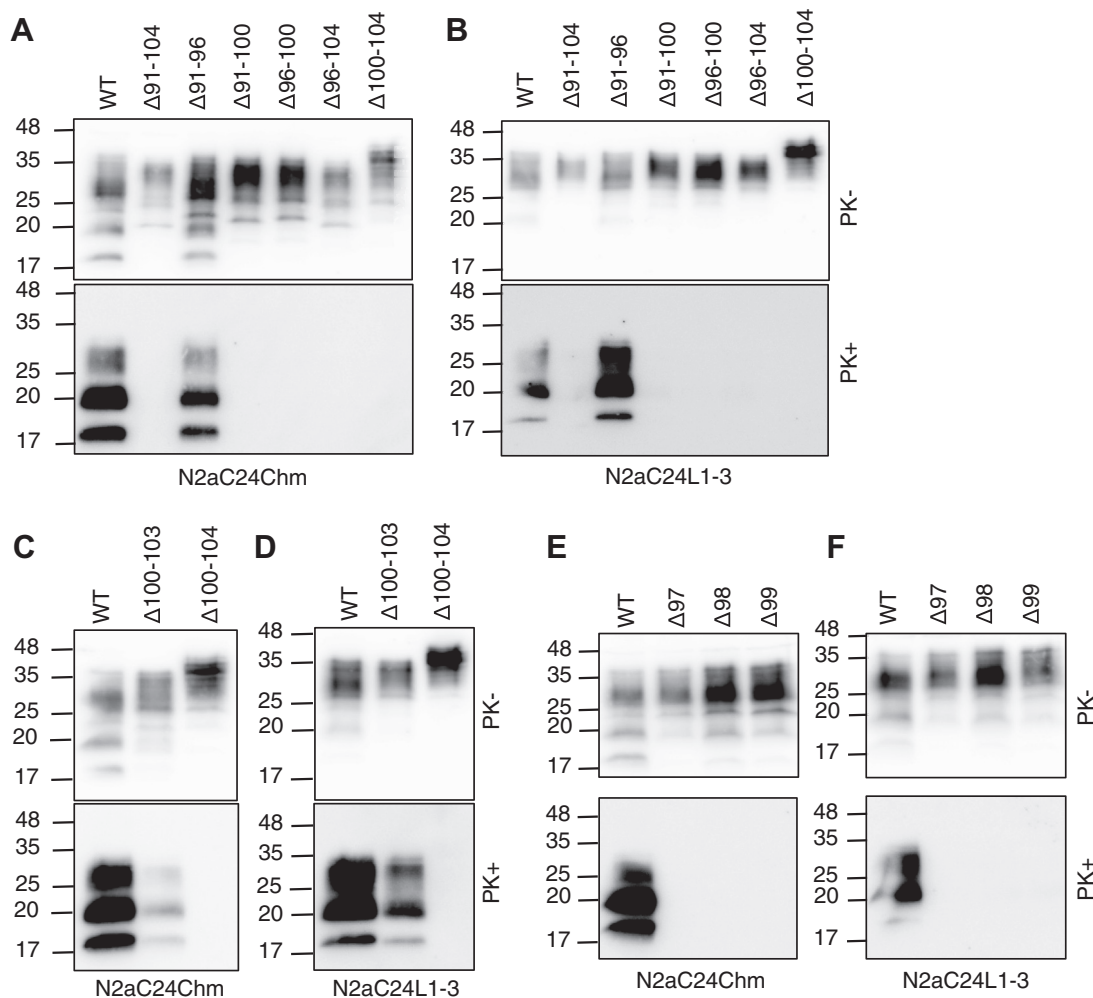


Figure 4. Crucial role of residues 97-99 in the conversion of PrP^C into PrP^{Sc} in RML- and 22L-infected cells. Western blotting with 3F4 anti-PrP antibody of cell lysates from N2aC24Chm (A) and N2aC24L1-3 cells (B) transduced with expression vectors encoding WT PrP^C(3F4), PrP Δ 91-104(3F4), PrP Δ 91-96(3F4), PrP Δ 91-100(3F4), PrP Δ 96-100(3F4), PrP Δ 96-104(3F4), and PrP Δ 100-104(3F4) after treatment with (+) or without (-) PK. Western blotting with 3F4 anti-PrP antibody of cell lysates from N2aC24Chm (C) and N2aC24L1-3 cells (D) transduced with expression vectors encoding WT PrP^C(3F4), PrP Δ 100-104(3F4), and PrP Δ 100-103(3F4) after with (+) or without (-) PK. Western blotting with 3F4 anti-PrP antibody of cell lysates from N2aC24Chm (E) and N2aC24L1-3 cells (F) transduced with expression vectors encoding WT PrP^C(3F4), PrP Δ 97(3F4), PrP Δ 98(3F4), and PrP Δ 99(3F4) after treatment with (+) or without (-) PK.

converted into PrP^{Sc} Δ 97-99 only after incubation with BSE-infected homogenates, but not with RML-, 22L-, and FK-1-infected homogenates (Fig. 5). No PrP^{Sc} and PrP^{Sc} Δ 97-99 was produced from WT PrP and PrP Δ 97-99, respectively, when incubated with prion-uninfected control brain homogenates (Fig. 5). These results suggest that residues 97-99 are important for the conversion of PrP^C into PrP^{Sc} in infection with RML, 22L, and FK-1 prions but not BSE prions.

Characterization of residues 97-99 important for PrP^C to convert into PrP^{Sc} after infection with RML and 22L prions

To further investigate the role of residues 97-99 in the conversion of PrP^C into PrP^{Sc} following infection with RML and 22L prions, we characterized the biochemical properties of residues 97-99 important for the conversion of PrP^C into PrP^{Sc} in RML- and 22L-infected cells. To do this, we transduced a series of PrP mutants with glutamine (Q) at position 97, tryptophan (W) at 98, and asparagine (N) at 99 mutated to

various residues, such as negatively charged glutamate (E) and aspartate (D), positively charged arginine (R), hydrophobic alanine (A), and nonpolar proline (P) into N2aC24Chm and N2aC24L1-3 cells. PrP mutants with charged residues at position 97, termed PrPQ97E(3F4), PrPQ97R(3F4), and PrPQ97D(3F4), completely lost their converting activity into PrP^{Sc}. However, a PrP mutant with hydrophobic alanine residue at position 97, PrPQ97A(3F4), was converted into PrP^{Sc}Q97A(3F4) at very low levels (Fig. 6A). PrP molecules with mutations at position 98, such as PrPW98E(3F4), PrPW98R(3F4), PrPW98D(3F4), and PrPW98A(3F4), were converted into PrP^{Sc} at low but easily detectable levels (Fig. 6B). PrPN99A(3F4) was also converted to PrP^{Sc}N99A(3F4) at low but easily detectable levels (Fig. 6C). However, no or very low levels of PrP^{Sc} was produced from PrPN99E(3F4), PrPN99R(3F4), and PrPN99D(3F4), all of which contain negatively or positively charged residues at position 99 (Fig. 6C). Furthermore, PrP mutants with proline residue at each position of residues 97-99, termed

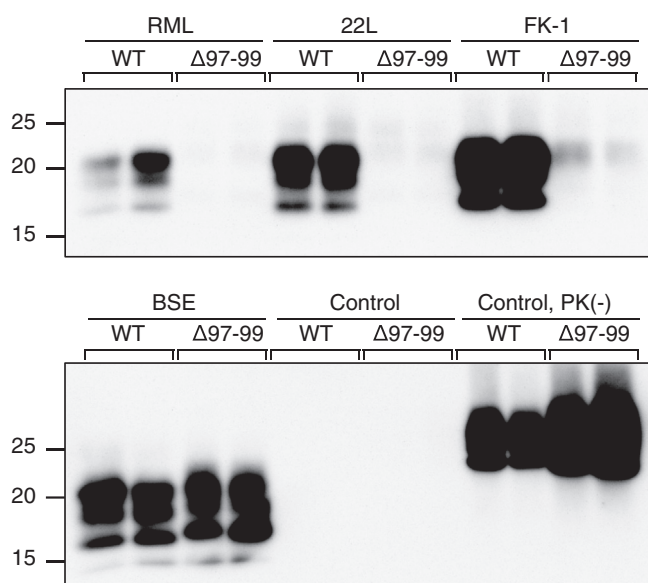


Figure 5. PMCA assay of WT PrP and PrP Δ 97-99 with RML, 22L, FK-1, and BSE prions. Western blotting of the first round PMCA products with or without PK treatment. PMCA was performed by incubating baculovirus-derived recombinant WT PrP or PrP Δ 97-99 with brain homogenates from RML-, 22L-, FK-1-, and BSE-infected WT mice and control prion-uninfected WT mice. BSE, bovine spongiform encephalopathy; PMCA, protein misfolding cyclic amplification.

PrPQ97P(3F4), PrPW98P(3F4), and PrPN99P(3F4), failed to convert into PrP^{Sc} (Fig. 6, A–C). These results indicate that mutations with proline residue at positions 97 to 99 and charged residues at positions 97 and 99 completely or almost completely destroyed the converting ability of the mutant PrPs into PrP^{Sc}, suggesting that the structural flexibility with non-charged properties of residues 97-99 might be important for the conversion of PrP^C into PrP^{Sc} after infection with RML and 22L prions.

Discussion

We previously reported that Tg(PrP Δ 91-106)/Prnp^{0/0} mice, which express PrP Δ 91-106 in their brains as low as 0.4-fold levels of PrP^C in WT mice, were resistant to RML, 22L, and FK-1 prions and only very poorly susceptible to BSE prions. In the present study, we generated a new line of Tg(PrP Δ 91-106)/Prnp^{0/0} mice, termed Tg(PrP Δ 91-106)-8545/Prnp^{0/0} mice, which overexpress PrP Δ 91-106 in their brains at levels 6-times higher than PrP^C in WT mice and showed that they remained healthy after intracerebral inoculation with RML, 22L, and FK-1 prions, without PrP^{Sc} Δ 91-106 in their brains except for one 22L-inoculated mouse accumulating very small amounts of PrP^{Sc} Δ 91-106 in its brain but developed disease earlier than WT mice after inoculation with BSE prions, with accumulation of PrP^{Sc} Δ 91-106 in their brains. These results clearly indicate that residues 91-106 are crucial for PrP^C to convert into PrP^{Sc} in infection with RML, 22L, and FK-1 prions but not BSE prions, therefore supporting infection with RML, 22L, and FK-1 prions but not BSE prions.

Tg(PrP Δ 91-106)-8545/Prnp^{0/0} mice accumulated PK-resistant PrP^{Sc} Δ 91-106 in their brains at levels lower than PK-resistant

PrP^{Sc} in control WT mice after inoculation with BSE prions. However, BSE-inoculated Tg(PrP Δ 91-106)-8545/Prnp^{0/0} mice developed disease earlier than control WT mice. Similar discrepancy between the levels of PK-resistant PrP^{Sc} and the length of incubation times has been reported in Tg mice overexpressing WT PrP^C after infection with RML prions (7). Compared to control WT mice, the Tg mice developed disease with shorter incubation times but accumulated less PK-resistant PrP^{Sc} in their brains (7). It is thus conceivable that the overexpression of PrP Δ 91-106, not the lack of residues 91-106, could be responsible for the lower brain accumulation of PK-resistant PrP^{Sc} Δ 91-106 and the shorter incubation times in BSE-inoculated Tg(PrP Δ 91-106)-8545/Prnp^{0/0} mice. It has been suggested that PrP^{Sc} molecules are heterogenous in their PK-resistance, including not only PK-resistant but also PK-sensitive PrP^{Sc} species (19, 20). It was shown that PK-resistant and PK-sensitive PrP^{Sc} molecules were both toxic to primary neurons (20). Thus, the overexpression of PrP Δ 91-106 might increase production of PK-sensitive, neurotoxic PrP^{Sc} Δ 91-106 species in BSE-infected Tg(PrP Δ 91-106)-8545/Prnp^{0/0} mice, therefore accelerating disease in these mice.

We showed that PrP Δ 91-104(3F4) failed to convert into PrP^{Sc} Δ 91-104(3F4) in N2aC24Chm and N2aC24L1-3 cells. Western blotting with SAF61 anti-PrP antibody, which recognizes endogenous PrP^C and PrP Δ 91-104(3F4), showed that compared to PrP^{Sc} in empty vector- or WT PrP^C(3F4)-transduced N2aC24Chm cells, it was significantly reduced in PrP Δ 91-104(3F4)-transduced N2aC24Chm cells in a manner dependent on the expression levels of PrP Δ 91-104(3F4). Consistent with this, PrP Δ 91-104(3F4)-transduced N2aC24L1-3 cells, which expressed the lower levels of PrP Δ 91-104(3F4), did not show PrP^{Sc} reduction. These results suggest that PrP Δ 91-104(3F4) might have a transdominant-negative inhibitory activity against the conversion of endogenous PrP^C into PrP^{Sc} in an expression level-dependent manner. It is thus possible that PrP Δ 91-106 might also have an inhibitory activity against the conversion of endogenous PrP^C into PrP^{Sc} in a transdominant-negative way.

PrP^C consists of two structural domains; the flexible, unstructured N-terminal domain, which includes residues 91-106, and the α -helix-rich, globular C-terminal domain (21, 22). Upon conversion into PrP^{Sc}, PrP^C undergoes marked conformational changes in the 2/3 C-terminal part to form a PK-resistant structure (23, 24). RML-, 22L-, and FK-1-PrP^{Sc}s have a PK cleavage site around residues 90 (25), thus residues 91-106 are entirely included in their PK-resistant structures. In contrast, BSE-PrP^{Sc} has a major PK cleavage site between residues 95 and 96 (26), indicating that residues 91-106 are only partially included in its PK-resistant structure. It is thus possible that residues 91-106 in PrP^C might be involved in the formation of the PK-resistant structure of RML-, 22L-, and FK-1-PrP^{Sc}s but not BSE-PrP^{Sc}, therefore Tg(PrP Δ 91-106)/Prnp^{0/0} mice being highly resistant to RML, 22L, and FK-1 prions but still susceptible to BSE prions.

PrP^{Sc} is abundant in β -sheet contents, in contrast to α -helix-rich PrP^C, suggesting that the structural transition of α -helices to β -sheets may be a key mechanism underlying the conversion of PrP^C into PrP^{Sc}. According to the cryo-electron microscopic analysis of PrP^{Sc} fibrils from 263K scrapie

Central residues crucial for prion protein conversion

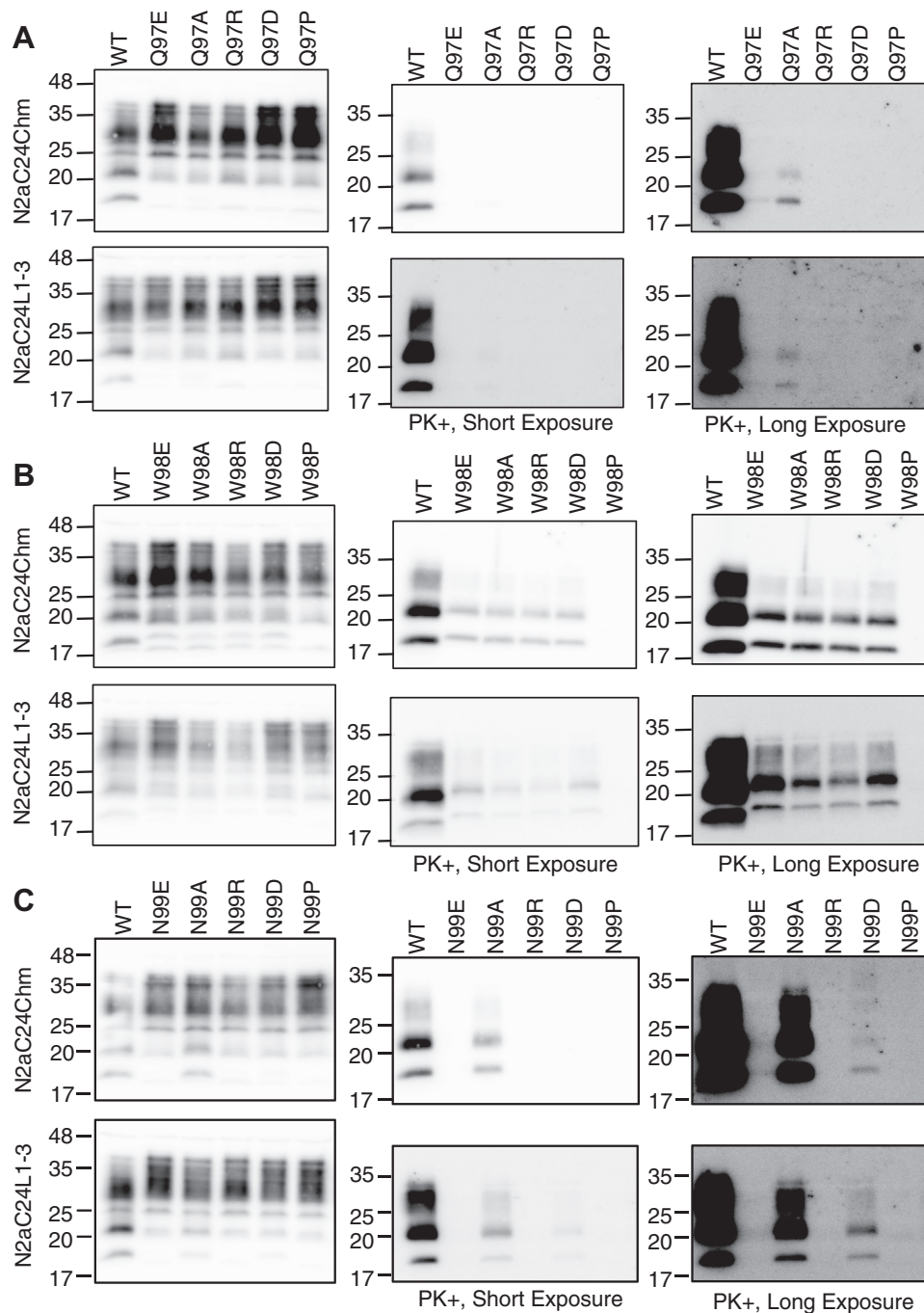


Figure 6. Characterization of residues 97–99 important for the conversion of PrP^C into PrP^{Sc} in RML- and 22L-infected cells. A, Western blotting with 3F4 anti-PrP antibody of cell lysates from N2aC24Chm and N2aC24L1-3 cells transduced with expression vectors encoding WT PrP^C(3F4), PrPQ97E(3F4), PrPQ97A(3F4), PrPQ97R(3F4), PrPQ97D(3F4), and PrPQ97P(3F4) after treatment with (+) or without (–) PK. B, Western blotting with 3F4 anti-PrP antibody of cell lysates from N2aC24Chm and N2aC24L1-3 cells transduced with expression vectors encoding WT PrP^C(3F4), PrPW98E(3F4), PrPW98A(3F4), PrPW98R(3F4), PrPW98D(3F4), and PrPW98P(3F4) after treatment with (+) or without (–) PK. C, Western blotting with 3F4 anti-PrP antibody of cell lysates from N2aC24Chm and N2aC24L1-3 cells transduced with expression vectors encoding WT PrP^C(3F4), PrPN99E(3F4), PrPN99A(3F4), PrPN99R(3F4), PrPN99D(3F4), and PrPN99P(3F4) after treatment with (+) or without (–) PK.

prion-infected hamster brains and RML-infected brains of transgenic mice expressing a glycosylphosphatidylinositol-anchorless PrP, PrP^{Sc} contained many β -sheets and assembled with parallel in-register intermolecular β -sheet structure to form the fibrils (27). Other investigators also carried out cryo-electron microscopic analysis for RML-PrP^{Sc} purified from the brains of RML-infected WT mice, reporting a similar

parallel in-register intermolecular β -sheet structure for RML-PrP^{Sc} (28). In RML-PrP^{Sc}, residues 95–99 formed the first β -sheet in the PK-resistant structure (28), indicating that residues 91–106 are essential for the formation of the first β -sheet in RML-PrP^{Sc}. Given that Tg(PrP Δ 91–106)/Prnp^{0/0} mice were resistant to RML, 22L, and FK-1 prions but not to BSE prions, it is possible that the formation of the first β -sheet might be

important for the conversion of PrP^C into PrP^{Sc} following infection with RML, 22L, and FK-1 prions but not BSE prions. Consistent with this concept, we found that PrP mutants lacking residues 97-99, which comprise a large part of the first β -sheet of residues 95-99, failed to convert into PrP^{Sc} in RML-infected N2aC24Chm and 22L-infected N2aC24L1-3 cells. We also found that recombinant PrP lacking residues 97-99 completely or almost completely lost the converting activity into PrP^{Sc} Δ 97-99 after incubation with RML-, 22L-, or FK-1-infected brain homogenates but almost fully converted into PrP^{Sc} Δ 97-99 with BSE-infected brain homogenates in an *in vitro* PMCA assay.

We showed that mutant PrPs, which carry proline residue at positions 97 to 99 or charged residues at positions 97 and 99, failed to convert into PrP^{Sc} or markedly reduced their converting ability into PrP^{Sc} in N2aC24Chm and N2aC24L1-3 cells. Proline is a unique residue with a covalent bond between the carbon in the side chain and the backbone nitrogen, forming a cyclic ring that imposes rigid constraints on a peptide bond and thereby reducing the structural flexibility of the surrounding region. It is thus possible that the structural flexibility of residues 97-99 and noncharged properties of positions 97 and 99 may be important for the formation of the first β -sheet upon the conversion of PrP^C into PrP^{Sc} after infection with RML and 22L prions. On the other hand, residue 95 is not included in the PK-resistant structure of BSE-PrP^{Sc} (26), suggesting that residues 95-99 might not form a β -sheet in BSE-PrP^{Sc}, therefore residues 97-99 being dispensable for the conversion of PrP^C into PrP^{Sc} following infection with BSE prions. The conformational selection model postulates that inoculated PrP^{Sc} could select host PrP^C as a substrate for conversion on the basis of its conformational compatibility with the host PrP^C (23, 24). It is thus alternatively possible that residues 91-106 or residues 97-99 might be important for PrP^C to adopt the conformation that is compatible with that of RML-, 22L-, and FK-1-PrP^{Sc}. However, BSE-PrP^{Sc} could be still structurally compatible even with PrP lacking residues 91-106.

Many anti-PrP antibodies have been reported to exhibit antiprion activities, clearing both PrP^{Sc} and prion infectivity from persistently infected cultured cells and preventing disease progression in animal models of acquired prion diseases (17, 29, 30), giving rise to the possibility of immunotherapeutics against prion diseases. 6D11 anti-PrP antibody, whose epitope (residues 97–100) includes residues 97-99, was also shown to have an antiprion activity, reducing PrP^{Sc} levels in 22L-infected N2a cells and in the spleens of 22L-infected mice (31–33). It has been suggested that 6D11 antibody might prevent the intermolecular interaction between PrP^C and PrP^{Sc} or the interaction of PrP^C with a yet unidentified molecule that is important for its conversion into PrP^{Sc} (31) or might target PrP^{Sc} for lysosomal degradation (33), thereby eventually reducing PrP^{Sc} levels in prion-infected cells. Our results also suggest another possibility that 6D11 antibody could reduce the structural flexibility of residues 97-99 by binding to its epitope, thereby preventing the conversion of PrP^C into PrP^{Sc} in prion-infected cells. Thus, agents capable of reducing the

structural flexibility of residues 97-99 and consequently disturbing the formation of the first β -sheet upon the conversion of PrP^C into PrP^{Sc} might be therapeutic against prion diseases, in which residues 97-99 play an important role in the conversion of PrP^C into PrP^{Sc}. In sporadic CJD of humans, two different types of PrP^{Sc} with distinct PK-cleavage site, termed PrP^{Sc} types 1 and 2, have been identified (34, 35). PrP^{Sc} type 1 is cleaved between residues 81 and 82 and PrP^{Sc} type 2 between 96 and 97 (34, 35). It is thus possible that residues 95-99 might form a β -sheet in PrP^{Sc} type 1 but not in PrP^{Sc} type 2, and also that residues 97-99-targeting agents might be therapeutically effective against PrP^{Sc} type 1-associated sporadic CJD.

In short, we showed here that residues 91-106 are crucial for PrP^C to convert into PrP^{Sc} after infection with RML, 22L, and FK-1 prions but not BSE prions in mice. We also showed that using RML- and 22L-infected cells, residues 97-99 are particularly important for PrP^C to convert into PrP^{Sc} in infection with RML and 22L prions probably through their structural flexibility with noncharged properties. An *in vitro* PMCA assay also supported the important role of residues 97-99 in the conversion of PrP^C into PrP^{Sc} in infection with RML, 22L, and FK-1 prions but not with BSE prions. Further elucidation of the exact role of residues 97-99 in the conversion of PrP^C into PrP^{Sc} could be helpful for understanding of the PrP conversion mechanism and the development of therapeutics against prion diseases.

Experimental procedures

Ethics statements

The Ethics Committees of Animal Care and Experimentation of the University of Occupational and Environmental Health (approval number AE08–013, March 18, 2019) approved this study. Animals were cared for in accordance with The Guiding Principle for Animal Care and Experimentation of the University of Occupational and Environmental Health and Japanese Law for Animal Welfare and Care. Every effort was made to reduce distress and the number of animals used.

Generation of Tg(PrP Δ 91-106)-8545/Prnp^{0/0} mice

The transgene used for Tg(PrP Δ 91-106)-8545/Prnp^{0/0} mice was constructed in elsewhere (12). In brief, a DNA fragment encoding mouse PrP Δ 91-106 was first constructed using polymerase chain reaction (PCR) and then inserted into a unique *Sal* I site of the Syrian hamster PrP cosmid vector, CosSHa.tet (InPro Biotechnology, Inc) to enable PrP Δ 91-106 to be expressed under the control of the promoter/enhancer of the hamster *Prnp*. The transgene was injected into the zygotes of Prnp^{0/0} mice, as described elsewhere (36, 37), after the removal of the cosmid-derived sequences, resulting in a line of Tg(PrP Δ 91-106)-8545/Prnp^{0/0} mice. Genotyping was performed by PCR as described elsewhere (38).

Prion inoculation

10% brain homogenates (w/v) were first prepared in phosphate-buffered saline (PBS) by passing brains from

Central residues crucial for prion protein conversion

terminally ill C57BL/6 mice infected with RML, 22L, FK-1, and BSE prions through 18 to 26 gauge needles and then diluted to 1% with PBS. A 20 μ l-aliquot of the homogenates was intracerebrally inoculated into 4- to 5-week-old Tg(PrP Δ 91-106)-8545/Prnp^{0/0} and C57BL/6 mice (CLEA Japan). Mice were diagnosed as disease when they developed more than five of the following clinical signs: emaciation, decreased locomotion, ruffled body hair, ataxic gait, kyphosis, priapism, upright tail, and paralysis of the hind legs, as described elsewhere (39).

Construction of expression vectors

DNA fragments encoding the N-terminal parts of mutant mouse PrPs with the 3F4 epitope were first amplified by PCR with a sense primer BamHI-PrP(ATG)-S (Table 2) and specific antisense primers (Table 2) using 3F4-tagged mouse WT PrP^C-encoding pcDNA3.1-moPrP(3F4) (40) as a template. Together with an antisense primer PrP(stop)-XbaI-AS

(Table 2), the resulting DNA fragments were then utilized as a 5' primer to amplify DNA fragments encoding full-length 3F4-tagged mutant PrPs using pcDNA3.1-moPrP(3F4) as a template. After DNA sequence confirmation, the amplified DNA fragments were inserted into BamHI I/Xba I-digested pcDNA3.1(+) (Invitrogen).

For the construction of a baculovirus expression vector for PrP Δ 97-99, pFastBac-moPrP Δ 97-99, a DNA fragment encoding the residues 1 to 96 fused with residues 100 to 104 of mouse PrP was first amplified by PCR with a Met forward sense primer (Table 2) and a PrP Δ 97-99-AS primer using pFastBac-moPrP (12) as a template. The resulting DNA fragment was then utilized as a 5' primer to amplify another DNA fragment encoding PrP Δ 97-99 together with a Stop reverse antisense primer (Table 2) using pFastBac-moPrP as a template. After DNA sequence confirmation of the fragment, they were inserted into BamHI I/Hind III-digested pFastBac1 (Thermo Scientific Inc), resulting in pFastBac-moPrP Δ 97-99.

Table 2
Primers and their sequences used for construction of the expression vectors in this study

Sense/antisense	Primer name	Sequence (5'→3')
Sense	BamHI-PrP(ATG)-S	<u>tcggatcc</u> cgctcatcatggcgaac (Underline, BamHI I; Bold, start codon)
Antisense	PrP(stop)-XbaI-AS	<u>ccttagag</u> ctcatcccacgatcag (Underline, Xba I; Bold, stop codon)
Specific antisense	PrP Δ 91-106-AS	<i>atgctcatg</i> ttttggcccat (Italic, downstream from codon 107; Not italic, upstream from codon 90)
	PrP Δ 91-105-AS	<i>cttcattg</i> ttttggcccat (Italic, downstream from codon 106; Not italic, upstream from codon 90)
	PrP Δ 91-104-AS	<i>catgtt</i> gtttttggcccat (Italic, downstream from codon 105; Not italic, upstream from codon 90)
	PrP Δ 91-96-AS	<i>ctgtccact</i> gtttggcccatcc (Italic, downstream from codon 97; Not italic, upstream from codon 90)
	PrP Δ 91-100-AS	<i>tggttct</i> gggtggcccatcc (Italic, downstream from codon 101; Not italic, upstream from codon 90)
	PrP Δ 96-100-AS	<i>tggttct</i> gggatgggtaccccc (Italic, downstream from codon 101; Not italic, upstream from codon 95)
	PrP Δ 96-104-AS	<i>catgtt</i> gtttttatgggtaccccc (Italic, downstream from codon 105; Not italic, upstream from codon 95)
	PrP Δ 100-104-AS	<i>catgtt</i> gtttttgtccactgatt (Italic, downstream from codon 105; Not italic, upstream from codon 99)
	PrP Δ 100-103-AS	<i>catgtt</i> gtttttgtccactgatt (Italic, downstream from codon 104; Not italic, upstream from codon 99)
	PrP Δ 97-AS	<i>gctggg</i> ctgttccaattatgggtaccccc (Italic, downstream from codon 98; Not italic, upstream from codon 96)
	PrP Δ 98-AS	<i>tttct</i> gggctgttctgattatgggtacc (Italic, downstream from codon 99; Not italic, upstream from codon 97)
	PrP Δ 99-AS	<i>tggtt</i> ctgggtccactgattatgggt (Italic, downstream from codon 100; Not italic, upstream from codon 98)
	PrP Δ 97-99-AS	<i>tggtt</i> ctgggtattatgggtaccccc (Italic, downstream from codon 100; Not italic, upstream from codon 96)
	PrPQ97E-AS	gggctt gttccattcattatgggtacc (Bold, mutated codon)
	PrPQ97A-AS	gggctt gttccaagcattatgggtacc (Bold, mutated codon)
	PrPQ97R-AS	gggctt gttccaagcattatgggtacc (Bold, mutated codon)
	PrPQ97D-AS	gggctt gttccaatcattatgggtacc (Bold, mutated codon)
	PrPQ97P-AS	gggctt gttccaaggattatgggtacc (Bold, mutated codon)
	PrPW98E-AS	gctggg ctgttttctgattatgggt (Bold, mutated codon)
	PrPW98A-AS	gctggg ctgttttagcctgattatgggt (Bold, mutated codon)
	PrPW98R-AS	gctggg ctgttttagcctgattatgggt (Bold, mutated codon)
	PrPW98D-AS	gctggg ctgtttatcctgattatgggt (Bold, mutated codon)
	PrPW98P-AS	gctggg ctgttttaggctgattatgggt (Bold, mutated codon)
	PrPN99E-AS	tttct gggctttccactgattatg (Bold, mutated codon)
	PrPN99A-AS	tttct gggcttagccactgattatg (Bold, mutated codon)
	PrPN99R-AS	tttct gggcttagccactgattatg (Bold, mutated codon)
	PrPN99D-AS	tttct gggcttagccactgattatg (Bold, mutated codon)
	PrPN99P-AS	tttct gggcttagccactgattatg (Bold, mutated codon)
	PrPK100E-AS	gtttct gggttcttccactgattat (Bold, mutated codon)
	PrPK100A-AS	gtttct gggagcgttccactgattat (Bold, mutated codon)
	PrPK100R-AS	gtttct gggacggttccactgattat (Bold, mutated codon)
	PrPK100D-AS	gtttct gggatcgttccactgattat (Bold, mutated codon)
	PrPK100P-AS	gtttct gggagggttccactgattat (Bold, mutated codon)
Primers for baculovirus expression vectors	Met forward sense primer	<u>cgagatcc</u> ccaccatggcgaactctgctac (underlined sequence, BamHI I site; bold sequence, start codon)
	Stop reverse antisense primer	<u>ccccagctt</u> catcccacgatcaggaag (underlined sequence, Hind III site; bold sequence, stop codon)
	PrP Δ 97-99-AS	<i>tggtt</i> ctgggtattatgggtaccccc (Italic, downstream from codon 100; Not italic, upstream from codon 96)

Protein misfolding cyclic amplification

Recombinant baculoviruses-derived WT PrP and PrP Δ 97-99 (Bac-WT PrP and Bac-PrP Δ 97-99) were purified by immobilized metal affinity chromatography (IMAC), as reported previously (41). In brief, pFastBac-moPrP and pFastBac-moPrP Δ 97-99 were first introduced into DH10 Bac *E. coli* and then transfected into *Spodoptera frugiperda* 21 insect cells with a bacmid DNA-Cellfectin mixture (Thermo Scientific Inc) to generate recombinant baculovirus encoding WT PrP or PrP Δ 97-99. The recombinant baculoviruses were then infected into High Five cells (Thermo Scientific Inc) for 72 h at 27 °C to produce Bac-WT PrP and Bac-PrP Δ 97-99, and the cell lysate was subjected to IMAC purification of Bac-WT PrP and Bac-PrP Δ 97-99. PMCA was then performed as described elsewhere (41). The PMCA reaction mixture was prepared by mixing 4 μ l of IMAC-purified Bac-WT PrP or PrP Δ 97-99 (approximately 100 ng/ μ l), 10 μ l of the PK- and heat-treated High Five cell lysate as a conversion inducer, 85 μ l of 1 \times PBS containing 4 mM EDTA and 0.25% Triton X-100, and 1 μ l of the 1% brain homogenates infected with RML, 22L, FK-1, and BSE prions. PMCA was performed using the automatic cross-ultrasonic protein activating apparatus (Elestein 070-GOT; Elekon Science Corp) as previously reported (41). Thirty-two cycles of sonication (pulse oscillation for 3 s was repeated five times at 0.1-s intervals) were followed by incubation at 37 °C for 30 min with gentle agitation. The resulting PMCA products were treated with 40 μ g/ml of PK for 1 h at 37 °C and subjected to Western blotting with horseradish peroxidase-conjugated T2 anti-PrP antibody, which recognizes residues 132-156 and 212-217 of mouse PrP (42). Signals were visualized using chemiluminescent detection reagent, EZWestLumi plus (ATTO) with a chemiluminescence imaging system (LuminoGraph I, ATTO).

Cell cultures

N2aC24L1-3 and NaC24Chm cells (43) were cultured in Dulbecco's Modified Eagle Medium High Glucose (Wako Pure Chemical Industries) supplemented with 10% heat-inactivated fetal bovine serum (Thermo Fisher Scientific) and 1 \times penicillin-streptomycin mixed solution (\times 100) (Wako Pure Chemical Industries). Cells were maintained in a 5% CO₂ in air humidified incubator at 37 °C and passaged at a 1:10 ratio every 3 to 4 days.

Transfection

N2aC24L1-3 and NaC24Chm cells were cultured in a 6-well plate at a density of 5 \times 10⁵ cells/well. Cells were transfected with 5 μ g plasmid DNA using Lipofectamine 2000 (Invitrogen) as recommended in the instruction manual. Two days later, the cells were lysed in lysis buffer (50 mM Tris-HCl, pH 7.4, 0.5% Triton X-100, 0.5% sodium deoxycholate, 150 mM NaCl, 2 mM EDTA) and microcentrifuged at 15,000 rpm for 5 min at 4 °C. The supernatants were subjected to protein concentration measurement using the bicinchoninic acid protein assay kit (Nacalai Tesque) and then to Western blotting.

Brain homogenization

Brain homogenates were prepared using a Multi-beads shocker (Yasui Kikai Co) in the lysis buffer and microcentrifuged at 3000 rpm for 5 min at 4 °C. The supernatants were subjected to protein concentration measurement using the bicinchoninic acid protein assay kit (Nacalai Tesque) and then to Western blotting.

Western blotting

For detection of PrP^{Sc}, brain homogenates and cell lysates treated with PK (20 μ g PK/mg proteins; Wako Pure Chemical Industries) at 37 °C for 30 min. Total proteins were separated by 15% SDS-polyacrylamide gels and then electrically transferred onto an Immobilon-P PVDF membrane (Millipore Corp). The membrane was blocked with 5% nonfat dry milk in TBST (0.5% Tween-20, 150 mM NaCl, 10 mM Tris-HCl, pH7.4) for 1 h at room temperature and then incubated with SAF61 mouse monoclonal antibody (Bertin Pharma), 3F4 mouse monoclonal anti-PrP antibody (BioLegend), IBL-N rabbit polyclonal anti-PrP antibodies (Immuno-Biological Laboratories), and anti-GAPDH antibody (Santa Cruz Biotechnology) overnight at 4 °C. After washed three times in TBST, the membrane was then incubated with HRP-conjugated anti-mouse IgG secondary antibody (GE Healthcare), anti-rabbit IgG antibody (GE Healthcare) in 1% nonfat dry milk-containing TBST for 1 h at room temperature. The immunoreactive signals were detected using Immobilon Western Chemiluminescent HRP substrate (Millipore) and a chemiluminescence image analyzer (LAS-4000 mini; Fujifilm Co). Densitometric analysis was performed using Image Gauge software (Fuji Film).

Data availability

All data are available in the main article or the supporting information.

Supporting information—This article contains supporting information.

Acknowledgments—We thank Stanley B. Prusiner for providing Prnp^{0/0} mice.

Author contributions—S. S. methodology; A. D. P., H. M., J. C., H. H., M. I., R. A., and S. S. investigation; A. D. P., H. M., J. C., H. H., M. I., R. A., and S. S. formal analysis; S. S. and A. D. P. writing-original draft.

Funding and additional information—This research was supported in part by JSPS KAKENHI (grand number 19H03548) to S. S. A. D. P. was supported by the OTSUKA Toshimi Scholarship Foundation (No. 20-66, No. 21-8).

Conflict of interests—The authors declare that they have no conflicts of interest with the contents of this article.

Abbreviations—The abbreviations used are: BSE, bovine spongiform encephalopathy; CJD, Creutzfeldt-Jakob disease; dpi, days

Central residues crucial for prion protein conversion

postinoculation; IMAC, immobilized metal affinity chromatography; PMCA, protein misfolding cyclic amplification.

References

1. Aguzzi, A., Baumann, F., and Bremer, J. (2008) The prion's elusive reason for being. *Annu. Rev. Neurosci.* **31**, 439–477
2. Prusiner, S. B. (1998) The prion diseases. *Brain Pathol.* **8**, 499–513
3. Bueler, H., Aguzzi, A., Sailer, A., Greiner, R. A., Autenried, P., Aguet, M., et al. (1993) Mice devoid of PrP are resistant to scrapie. *Cell* **73**, 1339–1347
4. Prusiner, S. B., Groth, D., Serban, A., Koehler, R., Foster, D., Torchia, M., et al. (1993) Ablation of the prion protein (PrP) gene in mice prevents scrapie and facilitates production of anti-PrP antibodies. *Proc. Natl. Acad. Sci. U. S. A.* **90**, 10608–10612
5. Manson, J. C., Clarke, A. R., McBride, P. A., McConnell, I., and Hope, J. (1994) PrP gene dosage determines the timing but not the final intensity or distribution of lesions in scrapie pathology. *Neurodegeneration* **3**, 331–340
6. Sakaguchi, S., Katamine, S., Shigematsu, K., Nakatani, A., Moriuchi, R., Nishida, N., et al. (1995) Accumulation of proteinase K-resistant prion protein (PrP) is restricted by the expression level of normal PrP in mice inoculated with a mouse-adapted strain of the Creutzfeldt-Jakob disease agent. *J. Virol.* **69**, 7586–7592
7. Fischer, M., Rulicke, T., Raeber, A., Sailer, A., Moser, M., Oesch, B., et al. (1996) Prion protein (PrP) with amino-proximal deletions restoring susceptibility of PrP knockout mice to scrapie. *EMBO J.* **15**, 1255–1264
8. Uchiyama, K., Miyata, H., Yano, M., Yamaguchi, Y., Imamura, M., Muramatsu, N., et al. (2014) Mouse-hamster chimeric prion protein (PrP) devoid of N-terminal residues 23–88 restores susceptibility to 22L prions, but not to RML prions in PrP-knockout mice. *PLoS One* **9**, e109737
9. Hara, H., Miyata, H., Das, N. R., Chida, J., Yoshimochi, T., Uchiyama, K., et al. (2018) Prion protein devoid of the octapeptide repeat region delays bovine spongiform encephalopathy pathogenesis in mice. *J. Virol.* **92**, e01368-17
10. Striebel, J. F., Race, B., Meade-White, K. D., LaCasse, R., and Chesebro, B. (2011) Strain specific resistance to murine scrapie associated with a naturally occurring human prion protein polymorphism at residue 171. *PLoS Pathog.* **7**, e1002275
11. Saijo, E., Kang, H. E., Bian, J., Bowling, K. G., Browning, S., Kim, S., et al. (2013) Epigenetic dominance of prion conformers. *PLoS Pathog.* **9**, e1003692
12. Uchiyama, K., Miyata, H., Yamaguchi, Y., Imamura, M., Okazaki, M., Pasiana, A. D., et al. (2020) Strain-dependent prion infection in mice expressing prion protein with deletion of central residues 91–106. *Int. J. Mol. Sci.* **21**, 7260
13. Feraudet, C., Morel, N., Simon, S., Volland, H., Frobert, Y., Creminon, C., et al. (2005) Screening of 145 anti-PrP monoclonal antibodies for their capacity to inhibit PrP^{Sc} replication in infected cells. *J. Biol. Chem.* **280**, 11247–11258
14. Fujita, K., Yamaguchi, Y., Mori, T., Muramatsu, N., Miyamoto, T., Yano, M., et al. (2011) Effects of a brain-engraftable microglial cell line expressing anti-prion scFv antibodies on survival times of mice infected with scrapie prions. *Cell Mol. Neurobiol.* **31**, 999–1008
15. Lund, C., Olsen, C. M., Tveit, H., and Tranulis, M. A. (2007) Characterization of the prion protein 3F4 epitope and its use as a molecular tag. *J. Neurosci. Met.* **165**, 183–190
16. Bosque, P. J., and Prusiner, S. B. (2000) Cultured cell sublines highly susceptible to prion infection. *J. Virol.* **74**, 4377–4386
17. Enari, M., Flechsig, E., and Weissmann, C. (2001) Scrapie prion protein accumulation by scrapie-infected neuroblastoma cells abrogated by exposure to a prion protein antibody. *Proc. Natl. Acad. Sci. U. S. A.* **98**, 9295–9299
18. Nishida, N., Harris, D. A., Vilette, D., Laude, H., Frobert, Y., Grassi, J., et al. (2000) Successful transmission of three mouse-adapted scrapie strains to murine neuroblastoma cell lines overexpressing wild-type mouse prion protein. *J. Virol.* **74**, 320–325
19. Cronier, S., Gros, N., Tattum, M. H., Jackson, G. S., Clarke, A. R., Collinge, J., et al. (2008) Detection and characterization of proteinase K-sensitive disease-related prion protein with thermolysin. *Biochem. J.* **416**, 297–305
20. Fang, C., Imberdis, T., Garza, M. C., Wille, H., and Harris, D. A. (2016) A neuronal culture system to detect prion synaptotoxicity. *PLoS Pathog.* **12**, e1005623
21. Riek, R., Hornemann, S., Wider, G., Glockshuber, R., and Wuthrich, K. (1997) NMR characterization of the full-length recombinant murine prion protein, mPrP(23–231). *FEBS Lett.* **413**, 282–288
22. Donne, D. G., Viles, J. H., Groth, D., Mehlhorn, I., James, T. L., Cohen, F. E., et al. (1997) Structure of the recombinant full-length hamster prion protein PrP(29–231): the N terminus is highly flexible. *Proc. Natl. Acad. Sci. U. S. A.* **94**, 13452–13457
23. Collinge, J., and Clarke, A. R. (2007) A general model of prion strains and their pathogenicity. *Science* **318**, 930–936
24. Wadsworth, J. D., Asante, E. A., and Collinge, J. (2010) Review: contribution of transgenic models to understanding human prion disease. *Neuropathol. Appl. Neurobiol.* **36**, 576–597
25. Mange, A., Beranger, F., Peoc'h, K., Onodera, T., Frobert, Y., and Lehmann, S. (2004) Alpha- and beta- cleavages of the amino-terminus of the cellular prion protein. *Biol. Cell* **96**, 125–132
26. Hayashi, H. K., Yokoyama, T., Takata, M., Iwamaru, Y., Imamura, M., Ushiki, Y. K., et al. (2005) The N-terminal cleavage site of PrP^{Sc} from BSE differs from that of PrP^{Sc} from scrapie. *Biochem. Biophys. Res. Commun.* **328**, 1024–1027
27. Kraus, A., Hoyt, F., Schwartz, C. L., Hansen, B., Artikis, E., Hughson, A. G., et al. (2021) High-resolution structure and strain comparison of infectious mammalian prions. *Mol. Cell* **81**, 4540–4551
28. [preprint] Manka, S. W., Zhang, W., Wenborn, A., Betts, J., Joiner, S., Saibil, H. R., et al. (2021) 2.7 Å cryo-EM structure of *ex vivo* RML prion fibrils. *bioRxiv*. <https://doi.org/10.1101/2021.12.13.472424>
29. White, A. R., Enever, P., Tayebi, M., Mushens, R., Linehan, J., Brandner, S., et al. (2003) Monoclonal antibodies inhibit prion replication and delay the development of prion disease. *Nature* **422**, 80–83
30. Peretz, D., Williamson, R. A., Kaneko, K., Vergara, J., Leclerc, E., Schmitt-Ulms, G., et al. (2001) Antibodies inhibit prion propagation and clear cell cultures of prion infectivity. *Nature* **412**, 739–743
31. Pankiewicz, J., Prelli, F., Sy, M. S., Kascsak, R. J., Kascsak, R. B., Spinner, D. S., et al. (2006) Clearance and prevention of prion infection in cell culture by anti-PrP antibodies. *Eur. J. Neurosci.* **23**, 2635–2647
32. Sadowski, M. J., Pankiewicz, J., Prelli, F., Scholtzova, H., Spinner, D. S., Kascsak, R. B., et al. (2009) Anti-PrP Mab 6D11 suppresses PrP(Sc) replication in prion infected myeloid precursor line FDC-P1/22L and in the lymphoreticular system *in vivo*. *Neurobiol. Dis.* **34**, 267–278
33. Pankiewicz, J. E., Sanchez, S., Kirshenbaum, K., Kascsak, R. B., Kascsak, R. J., and Sadowski, M. J. (2019) Anti-prion protein antibody 6D11 restores cellular proteostasis of prion protein through disrupting recycling propagation of PrP(Sc) and targeting PrP(Sc) for lysosomal degradation. *Mol. Neurobiol.* **56**, 2073–2091
34. Cali, I., Castellani, R., Alsheklee, A., Cohen, Y., Blevins, J., Yuan, J., et al. (2009) Co-Existence of scrapie prion protein types 1 and 2 in sporadic creutzfeldt-jakob disease: its effect on the phenotype and prion-type characteristics. *Brain* **132**, 2643–2658
35. Notari, S., Strammiello, R., Capellari, S., Giese, A., Cescatti, M., Grassi, J., et al. (2008) Characterization of truncated forms of abnormal prion protein in Creutzfeldt-Jakob disease. *J. Biol. Chem.* **283**, 30557–30565
36. Brinster, R. L., Chen, H. Y., Trumbauer, M. E., Yagle, M. K., and Palmiter, R. D. (1985) Factors affecting the efficiency of introducing foreign DNA into mice by microinjecting eggs. *Proc. Natl. Acad. Sci. U. S. A.* **82**, 4438–4442
37. Wilmut, I., Hooper, M. L., and Simons, J. P. (1991) Genetic manipulation of mammals and its application in reproductive biology. *J. Reprod. Fertil.* **92**, 245–279
38. Nishida, N., Tremblay, P., Sugimoto, T., Shigematsu, K., Shirabe, S., Petromilli, C., et al. (1999) A mouse prion protein transgene rescues mice deficient for the prion protein gene from purkinje cell degeneration and demyelination. *Lab. Invest.* **79**, 689–697

39. Sakaguchi, S., Katamine, S., Yamanouchi, K., Kishikawa, M., Moriuchi, R., Yasukawa, N., *et al.* (1993) Kinetics of infectivity are dissociated from PrP accumulation in salivary glands of Creutzfeldt-Jakob disease agent-inoculated mice. *J. Gen. Virol.* **74**, 2117–2123
40. Yamaguchi, Y., Miyata, H., Uchiyama, K., Ootsuyama, A., Inubushi, S., Mori, T., *et al.* (2012) Biological and biochemical characterization of mice expressing prion protein devoid of the octapeptide repeat region after infection with prions. *PLoS One* **7**, e43540
41. Imamura, M., Kato, N., Okada, H., Yoshioka, M., Iwamaru, Y., Shimizu, Y., *et al.* (2013) Insect cell-derived cofactors become fully functional after proteinase K and heat treatment for high-fidelity amplification of glycosylphosphatidylinositol-anchored recombinant scrapie and BSE prion proteins. *PLoS One* **8**, e82538
42. Hayashi, H., Takata, M., Iwamaru, Y., Ushiki, Y., Kimura, K. M., Tagawa, Y., *et al.* (2004) Effect of tissue deterioration on postmortem BSE diagnosis by immunobiochemical detection of an abnormal isoform of prion protein. *J. Vet. Med. Sci.* **66**, 515–520
43. Uchiyama, K., Muramatsu, N., Yano, M., Usui, T., Miyata, H., and Sakaguchi, S. (2013) Prions disturb post-Golgi trafficking of membrane proteins. *Nat. Commun.* **4**, 1846